ISSN 1068-798X, Russian Engineering Research, 2016, Vol. 36, No. 3, pp. 249–254. © Allerton Press, Inc., 2016.
Original Russian Text © A.V. Smirnov, D.I. Yushin, N.W. Solis Pinargote, P.Yu. Peretyagin, R. Torrecillas, 2015, published in STIN, 2015, No. 8, pp. 34–40.

Spark Plasma Sintering of Nanostructured Powder Materials

A. V. Smirnov[a], D. I. Yushin[a], N. W. Solis Pinargote[b], P. Yu. Peretyagin[a], and R. Torrecillas[a, b]

[a] *Stankin Moscow State Technical University, Moscow*
e-mail: smirnoff-andrey2009@yandex.ru, yushindenis@gmail.com, nw.solis@stankin.ru, p.peretyagin@stankin.ru, r.torrecillas@stankin.ru

[b] *Nanotechnology and Nanomaterials Research Center (CINN), Oviedo, Spain*
e-mail: director.cinn@csic.es

Abstract—Spark plasma sintering is a method of consolidating nanostructured powder materials and also composites and gradient materials in the presence of an electromagnetic field, by means of low-voltage sources of powerful current. The main benefit of spark plasma sintering is that previously impossible structures, properties, and compositions may be produced. The finite-element method is used to analyze the consolidation of samples by spark plasma sintering and by a hybrid method in which spark plasma sintering is combined with hot pressing. Corresponding numerical models are tested.

Keywords: spark plasma sintering, simulation, finite-element method, hot pressing, nanostructured powder materials

DOI: 10.3103/S1068798X16030163

INTRODUCTION

Nanostructured metals and ceramics are of great practical and scientific interest at present, on account of their distinctive properties. Accordingly, new methods and equipment for the machining of such materials are required [14–17, 20–25].

The most effective approach is spark plasma sintering, which involves the hot pressing of powder. A pulsing direct current permits rapid heating of the matrix and powder. Spark plasma sintering reduces the time for sample synthesis and improves the quality of the sintered material. In particular, nano- and submicrostructure may be retained in nanopowders on consolidation by this means.

In spark plasma sintering, heating involves passing pulsating direct current through the matrix and powder (Joule heating). Another option is hybrid heating, in which spark plasma sintering is combined with hot pressing based on inductive heating. This eliminates the temperature gradient in spark plasma sintering, which usually runs outward in the sample. The additional inductive element creates the opposite temperature gradient and thereby ensures a uniform temperature gradient over the cross section of the part.

However, the practical introduction of these methods is hindered by a lack of theoretical analysis. Our understanding of the physical processes within the powder on spark plasma sintering is insufficient for effective design and optimization of the process [18,19].

In the present work, we simulate the temperature and stress distribution within the part and matrix for spark plasma sintering in an FCT Systeme KCE-FCT H-HP D 25 system, with and without hot pressing.

To facilitate numerical modeling and finite-element analysis of spark plasma sintering and test the results, we create a simplified geometric model of the equipment. The properties of the materials employed are taken from literature sources [1–6, 13].

The following initial data (control parameters) are specified in creating a technological process for consolidation by spark plasma sintering (or hybrid sintering) on a FCT H-HP D 25 system: the sintering temperature of the sample (°C); the temperature of the mold (°C); the pressing force (kN); the sample's holding time at the sintering temperature (s); and the time of force application (s). For numerical modeling, other input data must be specified: the initial temperature of the sample, equipment, and chamber (°C); the direct current used in heating (A); the electrical voltage used in heating (V); the pressing force (kN) or pressure (Pa); and the time of current, voltage, force, or pressure application (s).

The data required for finite-element modeling are entered in the computer memory in the course of sintering. These data, which reflect the actual sintering process over time, are subsequently used to compare the results of finite-element modeling with experimental data and also to correct the numerical model. In Fig. 1, we show the data recorded in the consolidation of a sample (diameter 80 mm) from tungsten-carbide powder by the hybrid method (spark plasma sintering + hot pressing).

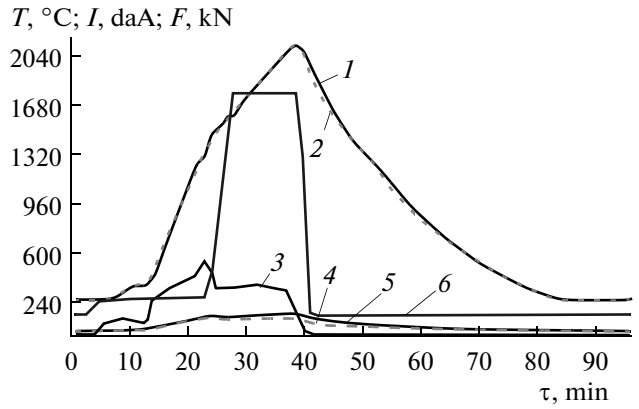

Fig. 1. Parameters for the hybrid sintering (spark plasma sintering + hot pressing) of a sample (diameter 80 mm) from tungsten-carbide (WC) powder: (*1*) upper pyrometer, temperature (°C); (*2*) lateral pyrometer, temperature (°C); (*3*) upper punch, temperature (°C); (*4*) lower punch, temperature (°C); (*5*) heating current (daA); (*6*) force (kN).

The theoretical model of powder consolidation by spark plasma sintering is based on partial differential equations describing the nonsteady heating and heat transfer in the associated thermoelectric problems; the stress–strain state of the system due to thermal expansion of the materials and the application of external pressure; and the compaction of the powder under the action of temperature and pressure.

The input control parameters for the model are the boundary conditions and the load. The properties of the equipment sample, which are entered in a file in the ANSYS library of materials, are also important input data, largely determining the outcome of modeling.

The boundary conditions in the model relate to the initial temperature (K), the vacuum-chamber volume (m^3), the emissivity of the system components, and the Stefan–Boltzmann constant ($W/(m^2 K^4)$).

The loads in the model (in thermoelectric analysis) are the direct current (A) and voltage (V).

This is a nonsteady model. An additional input parameter (prior to numerical modeling) is the time (s) of action of the load (current or voltage).

Besides numerical analysis of the distribution of mechanical and thermal stress in the equipment and the sample, this numerical model permits analysis of the stress–strain state of the whole system, since the distribution of mechanical and thermal strain may be calculated.

A finite-element model for powder sintering by the hybrid method (spark plasma sintering + hot pressing) is created on the basis of COMSOL Multiphysics software. By means of an interactive interface, that software permits the simulation of complex processes such as hybrid sintering, with the following components: Joule heating of the equipment (molds and punches) and the sample with passage of a large direct current

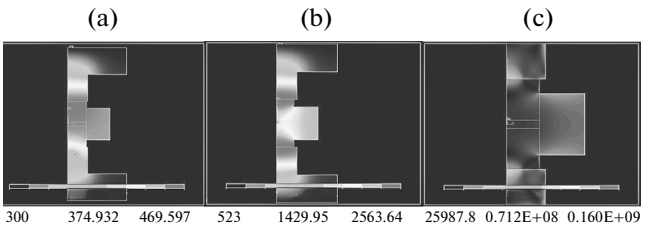

Fig. 2. Temperature distribution after 120-s passage of 1200 A (a) and 5000 A (b) with an initial temperature of 523 K; and mechanical-stress distribution when P = 394.7 kPa, after 120-s passage of 1200 A (c).

(heating by spark plasma sintering); inductive heating of the conductors by a cylindrical ac inductive heater (heating in hot pressing); the stress–strain state of the equipment and sample determined by the mechanical and thermal stress that arises in heating and pressing; and the compaction of the powder under the action of temperature and pressure.

In Fig. 2a, we show the temperature distribution in the model after passage of a 1200-A current for 120 s. The maximum temperature (750 K) is attained not in the sample or the mold but in the punches. This may be attributed to the high conductivity of tungsten carbide, as a result of which the current flows directly through the sample and intensely heats the punches and sample, beginning at the center. At the beginning of tungsten-carbide sintering, there is a considerable temperature gradient in the sample [7]. The modeling data are consistent with the experimental results in the memory of the system for spark plasma sintering (to within ±15–20%). This may be attributed to the following factors:

(1) the stored experimental data correspond to the hybrid process rather than to pure spark plasma sintering;

(2) the data on the properties of the equipment and the sample employed in modeling are mainly taken from literature sources and are not actual data regarding the properties of the specific materials employed in the experiment.

In Fig. 2b, we show the temperature distribution in the model after passage of a 5000-A current for 120 s. This corresponds to transition to the final stage of powder heating. As we see, the temperature distribution over the sample cross section is uniform; the discrepancy with the experimental data is no more than 10%.

Numerical analysis of Joule heating of the mold, punches, and powder in spark plasma sintering of tungsten carbide permits the determination of the distribution of mechanical and thermal stress in the model (Fig. 2c) [13].

The three-dimensional solid-state model of the system for hybrid sintering is shown in Fig. 3: it consists of graphite equipment for spark plasma sintering of samples (diameter 80 mm) and a copper cylindrical induction heater, separated from the graphite equip-

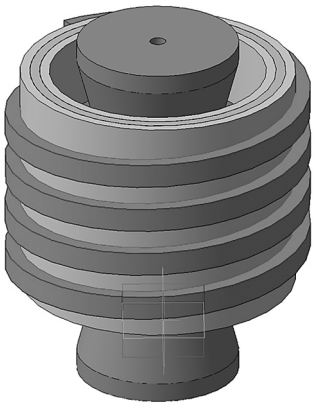

Fig. 3. Three-dimensional solid-state model of the system for hybrid sintering (spark plasma sintering + hot pressing).

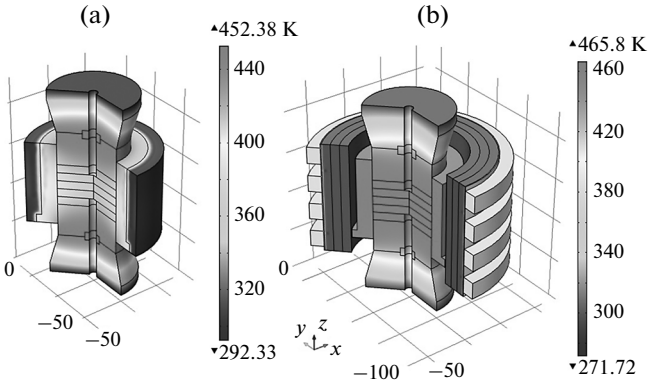

Fig. 4. Temperature distribution in the graphite equipment and sample for spark plasma sintering + hot pressing (a) and spark plasma sintering (b) with 100-s application of a current $I = 1500$ A.

ment by thermally and electrically insulating graphite felt. The solid-state model introduced in COMSOL Multiphysics software is a geometric model, to which a finite-element grid, boundary conditions, and loads are successively applied. The boundary conditions are the initial temperature of the model; the emissivity of the system components (the radiant heat losses in the vacuum chamber); and the attachment of the components of the graphite equipment and the inductive heating element.

In this model, the applied loads are the direct current supplied to the graphite electrodes; the alternating current supplied to the inductive element; and the pressure applied to the graphite punch.

The properties of the equipment and sample in the model are identical to those in the model of spark plasma sintering. The inductive element is made of copper; the properties of the heart-insulating graphite felt are taken from the standard COMSOL Multiphysics library of materials.

Test results of the model for hybrid sintering show considerable differences in the temperature distribution within the sample, punches, and mold. As we see in Fig. 4a, the hybrid method (spark plasma sintering + hot pressing) ensures a more uniform temperature distribution in the mold and the powder than in spark plasma sintering, which is characterized by a temperature gradient in ordinary conditions (Fig. 4b) [8, 9].

These results are consistent with those for the spark plasma sintering of a sample (diameter 80 mm) of tungsten-carbide powder (Fig. 1): practically identical temperature values are obtained from the upper pyrometer (measuring the temperature in the immediate vicinity of the powder) and the lateral pyrometer (measuring the temperature at the surface of the mold).

Researchers in various countries have studied the consolidation of complex samples from powder by spark plasma sintering. Two conceptual approaches may be identified by analysis of such research [10–12].

(1) Consolidation of a complex sample from powder in a mold of the required approach. Technical equipment with more than two punches or a system with two complex punches are used, depending on the complexity of the sample's shape.

(2) Production of the required sample by combining spark plasma sintering with extrusion or pressing. The initial blank is a presintered sample of simple shape [10].

However, these approaches require special equipment: punches and molds of specified size and shape.

The design of such special sintering tools is very challenging and has not been adequately studied. The basic requirements on the punches and molds for the sintering of complex samples are satisfactory consolidation of powder in direct sample formation (such that the size and density of the grains are the same or correspond to a gradient over the sample volume); and compatibility of the shaping load with the sample strength (for both approaches). Therefore, the design of punches and molds must include finite-element modeling for calculation of the sample strength and calculation of the thermal and electrical fields in consolidation.

In the present work, we create numerical models for finite-element analysis of the distribution of the temperature, current density, heat fluxes, and stress–strain state in the mold and sample, in the cases of spark plasma sintering and the hybrid method (spark plasma sintering + hot pressing). All the models are created and tested by means of COMSOL Multiphysics software.

The model of direct consolidation from powder (Fig. 5) corresponds to the sintering of samples in the form of rectangular and rhombic prisms, with rounding at the tips (analogous in geometry to standard lathe cutters), as well as samples of bush type.

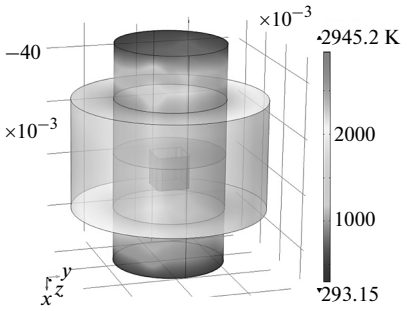

Fig. 5. Numerical model of the direct consolidation of a square WC plate by spark plasma sintering. $T = 120°C$.

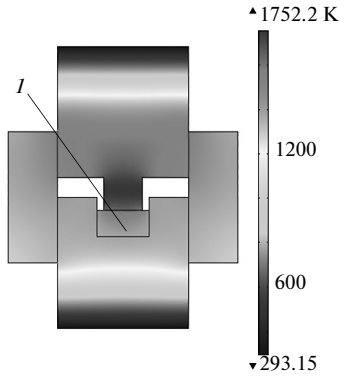

Fig. 6. Numerical model of the production of a TiAl-composite bush by spark plasma sintering + extrusion. $T = 60°C$.

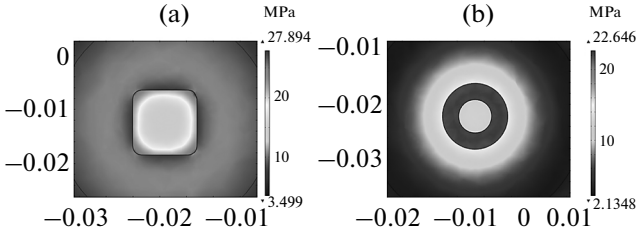

Fig. 7. Equivalent-stress distribution in the consolidation and shaping of a WC plate (a) and an Al_2O_3 bush (b). $T = 120°C$.

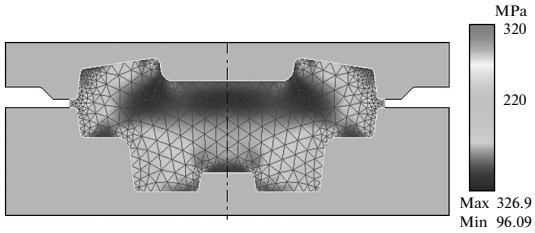

Fig. 8. Numerical modeling of the stress distribution in the spark plasma sintering of a presintered TiAl composite blank.

In these models, the punches and molds are made from the same graphite as in modeling the consolidation of tungsten carbide; the sample consists of pure tungsten carbide or pure aluminum oxide Al_2O_3.

The numerical model of the production of a complex sample from a presintered blank (Fig. 6) corresponds to shaping by spark plasma sintering and inverse pressing (extrusion) of sleeve samples from titanium and aluminum composite.

The calculation of the strength during the spark plasma sintering of complex samples is required to determine the shape and dimensions of the punches and molds and also to select or design the material used in the technological system. The most common calculation method is as follows: creation of a numerical model of sintering and shaping (or simultaneous sintering and shaping); finite-element simulation of the process and identification of the equivalent-stress distribution within the sample, punches, and molds; analysis of the stress state to find the stress concentrators and the maximum stresses (within the system elements); experimental verification; and comparison of the modeling results and experimental data.

Analysis of the numerical results for the stress state in the sintering of samples of tungsten-carbide and aluminum-oxide powder (square and rhombic plates and annular bushes) indicates that, in the given loading conditions, the stress in the complex punches does not exceed 30 MPa (Fig. 7).

This stress is considerably less than the strength of the graphite from which the laboratory punches and molds are made. At this stage, preparations are underway for experiments on the sintering and shaping of complex samples from powder and the parameter adjustment of the numerical models so as to permit correlation with practical data on spark plasma sintering.

The stress–strain state in the extrusion of a presintered blank heated by current transmission is characterized by larger stresses and strains than in combined consolidation and shaping (Fig. 8).

Finite-element models are created on the basis of COMSOL Multiphysics software for analysis of the temperature distribution in samples of specified shape and the corresponding equipment in spark plasma sintering (both hybrid consolidation and shaping and extrusion of a presintered blank). The system is heated by applying a direct current $I = 10000$ A for 120 s to a graphite punch–electrode. In Fig. 9, we show the temperature distribution in the sintering of 12 × 12 mm square plates (tip radius 1.6 mm) of tungsten carbide (a) and aluminum oxide (b).

In sintering plates of electrically conducting tungsten carbide, the maximum temperature of 2948 K appears in the sample and falls with steady gradient from the center of the sample to the graphite punch

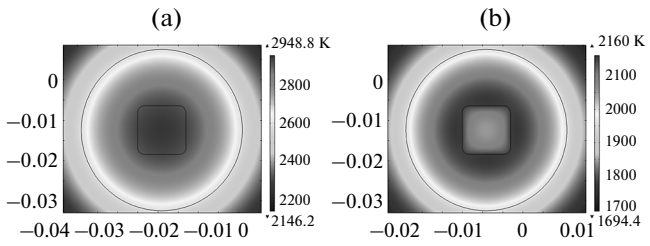

Fig. 9. Temperature distribution in the consolidation and shaping of a WC plate (a) and an Al_2O_3 plate (b).

(Fig. 9a). At the corners of the square, we observe the minimum sample temperature (around 2800 K). In the aluminum-oxide sample, we observe the opposite gradient and a lower maximum temperature (Fig. 9b). To reduce the temperature difference, we may use the hybrid method (spark plasma sintering + hot pressing) or more prolonged Joule heating.

CONCLUSIONS

(1) Finite-element modeling of the physical processes in the spark plasma sintering of nanostructured powder materials provides the following results.

(1.1) The creation of a numerical model of the spark plasma sintering of samples from tungsten-carbide powder by means of ANSYS software in APDL programming language.

(1.2) The creation of a numerical model of the hybrid sintering (spark plasma sintering + hot pressing) of samples from tungsten-carbide powder by means of COMSOL Multiphysics software.

(1.3) The development of numerical models of spark plasma sintering with the creation of samples of specified shape and size.

(1.4) Theoretical confirmation of the possibility of sintering samples of specified shape and size.

(2) The numerical models that have been developed may be used for the following purposes.

(2.1) Finite-element analysis of the distribution of mechanical and thermal stress in samples of tungsten carbide or other materials and also in the technological equipment at different stages of spark plasma sintering or the hybrid process (spark plasma sintering + hot pressing).

(2.2) Finite-element analysis of the density distribution in samples of tungsten carbide or other materials and also in the technological equipment at different stages of spark plasma sintering or the hybrid process (spark plasma sintering + hot pressing).

(2.3) Design, testing, and optimization of special equipment (molds and punches) for the consolidation of complex samples by spark plasma sintering or the hybrid process (spark plasma sintering + hot pressing).

(2.4) The design of technological equipment and half-molds for the production of nanocomposites with specified dimensions, in complete agreement with the requirements on manufacturing components.

ACKNOWLEDGMENTS

Financial support was provided by the Russian government (decree 220, April 9, 2010; contract 14.V25.31.0012, June 26, 2013).

REFERENCES

1. COMSOL Multiphysics v. 4.3a Material library.
2. Kolotyrkin, Ya.M. and Knyazheva, V.M., *Itogi Nauki i Tekhniki, Seriya: Korroziya i Zashchita ot Korrozii* (Achievements of Science and Technology, Corrosion and Corrosion Protection), Moscow: Vseross. Inst. Nauch. Tekh. Inform., Ross. Akad. Nauk, 1974, vol. 3.
3. Yang, H., Multi-field simulation of the spark plasma sintering process, *Thesis in Engineering Mechanics,* Philadelphia: Pa. State Univ., 2010.
4. Schunk–innovative insulation materials. http://www.ingenieurparadies.de/sixcms/media.php/1466/20_39e_Innovative_Insulation_Materials.pdf
5. Vanmeensel, K., Laptev, A., Hennicke, J., Vleugels, J., and van der Biest, O., Modeling of the temperature distribution during field assisted sintering, *Acta Mater.,* 2005, vol. 53, pp. 4379–4388.
6. http://www.ilma-sealing.com/file.php?Grafitovaya_folga_Sigraflex-gid-121-136-416.pdf
7. Tiwari, D., Basu, D., and Biswas, K., Simulation of thermal and electric field evolution during spark plasma sintering, *Ceram. Int.,* 2009, no. 35, pp. 699–708.
8. Vanmeensel, K., Laptev, A., van der Biest, O., and Vleugels, J., Field assisted sintering of electro-conductive ZrO_2-based composites, *J. Eur. Ceram. Soc.,* 2007, no. 27, pp. 979–985.
9. Zhang, J., Numerical simulation of thermoelectric phenomena in field activated sintering, PhD Thesis, Philadelphia, PA: Drexel Univ., 2004.
10. Khaleghi, E.A., Tailored net-shape powder composites by spark plasma sintering, *PhD Dissertation in Engineering Science,* San Diego, CA: Univ. of California, 2012.
11. Ruskola, M., Numerical modeling of pulsed electric current sintering process, *MSc Thesis in Technology,* Espoo, Finland: Aalto Univ., 2014.
12. Voisina, T., Duranda, L., Karnatakbat, N., Galletc, S.L., Thomasd, M., Le Berree, Y., Castagnef, J.F., and Coureta, A., Temperature control during spark plasma sintering and application to up-scaling and complex shaping, *J. Mater. Process. Technol.,* 2013, no. 213, pp. 269–278.
13. Wang, C., Cheng, L., and Zhao, Z., FEM analysis of the temperature and stress distribution in spark plasma sintering: modeling and experimental validation, *Comput. Mater. Sci.,* 2010, no. 49, pp. 351–362.
14. Dmitriev, A.M., Korobova, N.V., and Tolmachev, N.S., Experimental verification of the results of computer simulation of the stresses on the element of deforming tool, *Vestn. Mosk. Gos. Tekhnol. Univ., Stankin,* 2014, no. 2(29), pp. 44–49.

15. Kalyakulin, S.Yu. and Kuz'min, V.V., Development of mathematical model of technological process parameters, *Vestn. Mosk. Gos. Tekhnol. Univ., Stankin,* 2014, no. 3 (30), pp. 40–44.

16. Kabak, I.S., Neural network model for forecasting and assessment of software reliability, *Vestn. Mosk. Gos. Tekhnol. Univ., Stankin,* 2014, no. 1 (28), pp. 107–111.

17. Bolbukov, V.P., Regulation of the energy of fast gas atoms by change in the resistor strength, located between the working chamber and the emission grid of a source, *Vestn. Mosk. Gos. Tekhnol. Univ., Stankin,* 2014, no. 3 (30), pp. 54–57.

18. Sobolev, A.N., Kosov, M.G., and Nekrasov, A.Ya., Simulation of construction of the body parts using the estimated trace elements, *Vestn. Mosk. Gos. Tekhnol. Univ., Stankin,* 2014, no. 3 (30), pp. 98–101

19. Kozochkin, M.P. and Solis Pinargote, N.W., Analysis of the effects of vibration turning using coolants, *Vestn. Mosk. Gos. Tekhnol. Univ., Stankin,* 2014, no. 4 (31), pp. 67–73.

20. Frolov, E.B., Kryukov, V.V., and Kryukov, A.V., Integration of the systems of automated design of technological processes and operational industrial systems based on control database formation, *Vestn. Mosk. Gos. Tekhnol. Univ., Stankin,* 2014, no. 4 (31), pp. 133–139.

21. Grigor'ev, S.N., Kuzin, V.V., Fedorov, S.Yu., Tibor Szalay, and Balazs Farkas, Technological aspects of the electrical-discharge machining of small-diameter holes in a high-density ceramic. Part 1, *Refract. Ind. Ceram.,* 2014, vol. 55, no. 4, pp. 330–334.

22. Kuzin, V.V., Grigor'ev, S.N., and Ermolin, V.N., Stress inhomogeneity in a ceramic surface layer under action of an external load. Part 1. Effect of complex mechanical loading, *Refract. Ind. Ceram.,* 2014, vol. 54, no. 5, pp. 416–419.

23. Kuzin, V.V., Grigor'ev, S.N., and Ermolin, V.N., Stress inhomogeneity in a ceramic surface layer under action of an external load. Part 2. Effect of thermal loading, *Refract. Ind. Ceram.,* 2014, vol. 54, no. 6, pp. 497–501.

24. Kuzin, V.V., Grigor'ev, S.N., and Ermolin, V.N., Stress inhomogeneity in a ceramic surface layer under action of an external load. Part 3. Effect of a distributed force load, *Refract. Ind. Ceram.,* 2014, vol. 55, no. 1, pp. 36–39.

25. Kuzin, V.V., Grigor'ev, S.N., and Ermolin, V.N., Stress inhomogeneity in a ceramic surface layer under action of an external load. Part 4. Combined effect of force and thermal loads, *Refract. Ind. Ceram.,* 2014, vol. 55, no. 1, pp. 40–44.

Translated by Bernard Gilbert